drones

Article

Study on Drone Handover Methods Suitable for Multipath Interference Due to Obstacles

Kakeru Hirata [1], Takefumi Hiraguri [1,*], Tomotaka Kimura [2], Takahiro Matsuda [3], Tetsuro Imai [4], Jiro Hirokawa [5], Kazuki Maruta [6] and Satoshi Ujigawa [7]

1 Electronics, Information and Media Engineering Major, Nippon Institute of Technology, Saitama 345-8501, Japan; 2228014@stu.nit.ac.jp
2 Faculty of Science and Engineering, Doshisha University, Kyoto 610-0321, Japan; tomkimur@mail.doshisha.ac.jp
3 Graduate School of Systems Design, Tokyo Metropolitan University, Tokyo 191-0065, Japan; takahiro.m@tmu.ac.jp
4 School of Engineering, Tokyo Denki University, Tokyo 120-8551, Japan; imaite@mail.dendai.ac.jp
5 Department of Electrical and Electronic Engineering, Tokyo Institute of Technology, Tokyo 152-8550, Japan; jiro@ee.e.titech.ac.jp
6 Faculty of Engineering, Tokyo University of Science, Tokyo 125-8585, Japan; maruta@rs.tus.ac.jp
7 Kajima Technical Research Institute, Kajima Corporation, Tokyo 182-0036, Japan; ujigawa@kajima.com
* Correspondence: hira@nit.ac.jp

Abstract: Networks constructed in the sky are known as non-terrestrial networks (NTNs). As an example of an NTN, relay transmission using drones as radio stations enables flexible network construction in the air by performing handovers with ground stations. However, the presence of structures or obstacles in the flight path causes multipath interference; consequently, the propagation environment fluctuates significantly based on the flight. In such a communication environment, it is difficult for a drone to select an optimal ground station for a handover. Moreover, unlike a terrestrial network, the propagation environment of a flying drone is affected by structures and other factors that cause multipaths based on the flight speed and altitude, making the conditions of the propagation environment even more complex. To solve these problems, we propose handover schemes between drones and the ground that consider the multipath interference caused by obstacles. The proposed methods are used to perform handovers based on an optimal threshold of received power considering interference and avoid unnecessary handovers based on the moving speed, which makes the handover seamless. Finally, we develop a simulator that evaluates the cross layer from propagation to upper network protocols in a virtual space, including buildings, evaluate the communication quality of a drone flying in a three-dimensional space, and confirm the effectiveness of the proposed methods as well as the evaluation of the real environment.

Keywords: drones; handover; multipath interference; non-terrestrial networks

Citation: Hirata, K.; Hiraguri, T.; Kimura, T.; Matsuda, T.; Imai, T.; Hirokawa, J.; Maruta, K.; Ujigawa, S. Study on Drone Handover Methods Suitable for Multipath Interference Due to Obstacles. *Drones* **2024**, *8*, 32. https://doi.org/10.3390/drones8020032

Academic Editor: Emmanouel T. Michailidis

Received: 11 December 2023
Revised: 18 January 2024
Accepted: 20 January 2024
Published: 23 January 2024

1. Introduction

The fifth-generation (5G) [1] network was developed as a wireless network technology, and services using 5G provide attractive functions, such as communication speed, communication capacity, and user capacity. Additionally, design methods for the optimal installation of base stations and evaluation and verification methods for the multipath fading effects of interference and reflections caused by buildings and shields between base stations and users, propagation attenuation, and improvement methods have been established.

Beyond 5G and 6G, next-generation wireless network technologies have attracted attention. Beyond 5G and 6G include the requirement of extending the communication area to the sea, sky, and space, which is different from a terrestrial network [2–11]. Communication networks that satisfy these requirements are called non-terrestrial networks (NTN) [12–18]. As shown in Figure 1, satellites and relay stations, such as high-altitude

platform stations (HAPS), are placed in the sky, and drones and robots near the ground are expected to have various applications, such as information collection. In addition, unlike conventional network designs that approximate a flat surface on the ground, three-dimensional network construction that includes three-dimensional movement in the air offers high potential for creating new services due to the flexibility of the design. In the future, a shift toward NTNs linked to conventional ground networks is expected. Relay communication using drones has been proposed in conventional relayed networks when it is difficult to set up a ground station to expand the communication area or eliminate blind zones [19,20]; for example, research on relay transmission using drones and 5G technology already exists, and demonstrative experiments have been conducted [21]. For example, demonstration experiments have been reported for transmitting 4K high-resolution video shots from the sky using 5G, as shown in Figure 2. Moreover, transmission technology for coverage holes where wireless signals cannot reach directly are already in the process of being put to practical use.

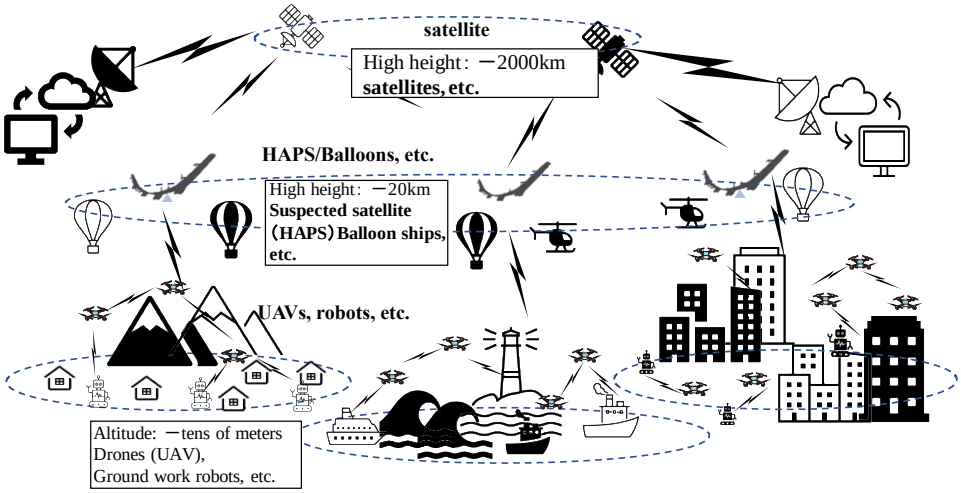

Figure 1. NTN image model configuration.

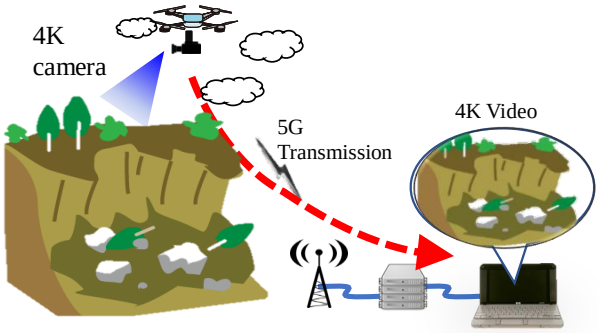

Figure 2. Relay transmission using drones.

However, although simple relaying by drones can be achieved, weight limitations make it impossible to carry heavy payloads, such as devices that transmit high-power radio waves or directional antennas, which makes it difficult to achieve a wide communication area. Moreover, because drones are mobile, no method has been proposed to exploit their ability to connect with various ground-based stations while moving. Furthermore, unlike terrestrial communications, it is necessary to consider three-dimensional propagation paths with height differences for drones to communicate with the ground and mobile stations. For example, multipath interference, diffraction, and shielding caused by reflections from structures vary greatly with the height of the structure and flying drone. Therefore, this study focused on airborne networks that use drones as radio stations. For example, as

shown in Figure 3, the network is expected to be used for capturing pictures, collecting oceanographic data, relaying between terminals and base stations with no line of sight, and providing a communication environment for users in blind areas. To realize such a network, it is desirable to assume that the drone moves while flying, and to switch connections so that it can continuously communicate while searching for the most appropriate base station on the ground during its movement. The method of switching the destination is called handover, and we propose a handover method suitable for drones. For the handover evaluation, we developed a cross-layer simulator that combines multiple analysis methods of the communication layer [22] to obtain the communication speed or throughput at the service level by combining the propagation characteristics in a three-dimensional (3D) space that considers structures and network protocols. In addition, we evaluated the proposed methods. The reason for developing the cross-layer simulator is that when a drone communicates while flying, unlike cellular communication, etc., on the ground, it is necessary to assume a three-dimensional communication environment. Reflections and diffraction of radio waves due to buildings and other obstacles vary in complexity that depends on the drone's flight altitude and speed. When considering the communication quality in such a communication environment, it is necessary to evaluate performance in a three-dimensional space considering the propagation characteristics. For cellular communications on the ground, the location selection of base stations are performed not only by computer simulation, but also by demonstration experiments to verify the optimal installation of base stations and the quality of communications. On the other hand, when the drones communicate while flying, the selection of base station locations by actually flying is a very labor-intensive and expensive task. Although computer simulations can evaluate propagation characteristics in a three-dimensional space, it is difficult to evaluate the performance and services of a communication system, including its applications. For this background, an evaluation method suitable for the environment of drone communications is required, and because verification through actual experiments is difficult, a virtual reality simulator for evaluation in a virtual space is needed. In this study, to achieve this simulator for evaluation, we developed the cross-layer simulator that integrates propagation characteristics, signal processing, and communication protocols such as an IP layer.

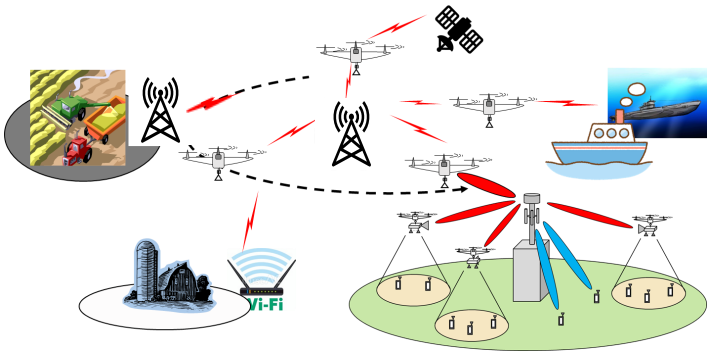

Figure 3. Example of service using a drone as a radio station.

The contributions of this paper are summarized as follows.

- We propose a handover method based on signal-to-interference-plus-noise ratio (SINR) that includes multipath interference considering obstacles such as buildings in the environment where drones fly, instead of simple received power. Then, the effectiveness of the method was confirmed.
- We proposed a method to solve the problem of locally high SINR during the period when drones are flying and the communication speed is reduced due to frequent handovers, confirmed the effectiveness of the method, and determined the optimal flight speed.
- Because drone communications are subject to significant changes in reflection and diffraction from buildings and other objects depending on flight speed, the new cross-

layer simulator was developed to determine throughput characteristics above the IP layer, including multipath interference due to propagation characteristics and signal processing performance, enabling evaluation in a three-dimensional virtual space close to the actual environment.

The remainder of this paper is organized as follows. Section 2 describes the related works and problems associated with conventional relay technology. Section 3 describes the evaluation method and simulator development for the drone relay network for flight. Section 4 describes the two proposed methods and presents evaluation results.

2. Related Work

2.1. Introduction of Relay Technology by Drone

In this study, we propose a handover method suitable for drones in flight. In wireless communication, a handover is a technique in which a moving radio station switches its destination and continues to communicate. The communication requires stabilizing the communication speed and achieving seamless switching. For example, a handover in IEEE802.11 standard [23] local area networks (LANs) is a method in which moving stations (STAs) switch connections from one access point (AP) to another and continue to communicate. Before performing a handover, STAs search for possible APs by scanning the surrounding APs for information such as the signal strength of the new AP. For example, STAs compare the APs to which they are currently connected and analyze whether the new AP can provide a stronger signal or whether communication speed can be improved. However, the functionality implemented in commercial devices generally searches for surrounding APs at the time of disconnection, and an optimal handover trigger selection method for seamless connections has not yet been established. When a suitable AP is found from the search results, an authorization process is performed between the STA and the new AP, and then an association is established. Communication with the previous AP is disconnected. In these handover procedures, the switchover should be seamless, and the STA should continue a certain amount of data communication with the new AP during the switchover. Finally, the new AP takes over the STA's communications and provides the same services as the previous AP.

Two types of roaming methods are specified in the IEEE802.11r standard [24–27] as roaming methods when handovers are performed. One is over-the-air fast transmission (FT) roaming, and the other is over-the-DS FT roaming. First, over-the-air FT roaming is explained using Figure 4. The STA requests roaming from AP1, to which it is connected (communicating with the access point). Subsequently, the STA sends an FT authentication request to AP2 and receives an FT authentication response from AP2. The controller connected to AP1 and AP2 sends the STA pre-certification information to AP2. Finally, when the STA moves to the BSS to which the new AP belongs, it sends an FT reconnection request to the STA and receives an FT reconnection response from AP2 to complete roaming. The operation of over-the-DS FT roaming is explained in Figure 5. First, the STA connects to AP1 and requests roaming to AP2. Subsequently, the STA sends an FT authentication request to AP1 and receives an FT authentication response from AP1. The controller connected to both AP1 and AP2 sends the STA pre-certification information to AP2. Finally, when the STA moves to the BSS to which the new AP belongs, it sends an FT reconnection request to the STA and receives an FT reconnection response from AP2 to complete roaming. These roaming methods solve the problem of the large overhead of the authentication procedure in handover: the over-the-DS FT performs authentication before switching the APs, and the over-the-DS FT can further reduce the number of authentication procedures in the wireless section by cooperating with the backbone network. The over-the-DS FT can further reduce the number of authentication steps in the wireless section by coordinating with the backbone network. In other words, this method can effectively reduce the authentication procedure time by deploying a controller. However, the methods for the STA to switch AP connections and select APs to connect to are not specified, and the effect of physical disconnection on seamless handover has not been considered. In this study, we discuss how

to select the optimal AP to connect to by minimizing the time spent on the handover of the switching decision mechanism and the protocol procedures involved in actual switching. More specifically, because the authentication procedure is not the subject of discussion, this study assumes the use of over-the-DS FT authentication, which is largely independent of the authentication time of the wireless segment and focuses on the seamlessness of the part where the wireless connection is physically switched.

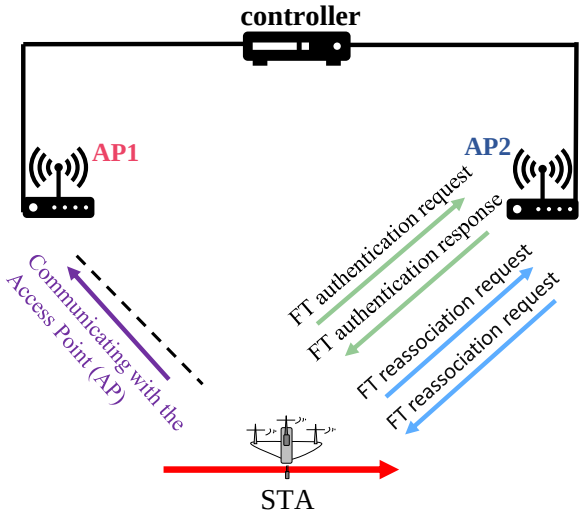

Figure 4. Over-the-air FT roaming.

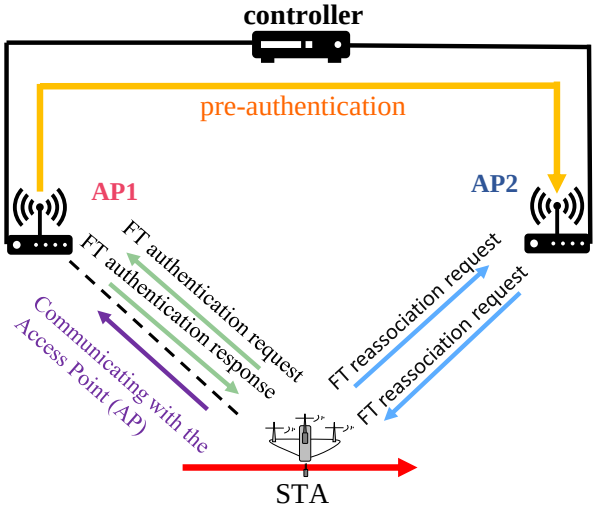

Figure 5. Over-the-DS FT roaming.

In addition, other work related to this study is presented. In relay methods that use drones, drones have been emphasized to improve the transmission rate and reduce the error rate [28]. The proposed method uses an uplink multi-user multiple input multiple output (MU-MIMO) cooperative retransmission control scheme. When the drones in flight communicate directly with each other, another drone, which cooperates and assists in communication based on the transmission distance, performs a relay transmission to guarantee transmission errors. The method guarantees transmission errors and achieves a transmission rate of 1.5 times even when there is considerable interference from the ground, and it is also expected to improve blind zones because it establishes relays over a wide area. In addition, in [29], the authors improved the communication capacity characteristics of MIMO systems using drone relay stations by introducing a propagation environment control method (PECM) that selects the best arrangement of drones from among multiple drones in a drone relay network. However, neither of these methods discusses how

drones move to the relay, and handovers by movement require different and new capabilities. Ad hoc networks that use drones were studied by [30]. In this research, when the communication infrastructure on the ground fails, such as during a disaster, unmanned aerial vehicles (UAVs), such as drones, can be deployed to provide a rapid communication environment for victims and emergency workers, efficiently delivering information in the disaster area even when the communication infrastructure is unavailable. However, handovers to ground stations have not been discussed. In these related studies, handover is beyond the scope, including the effects of the drone's maneuverability, movement speed, and obstacles, such as buildings.

In air-to-ground and air-to-air, communication channel characteristics are highly dynamic [31,32]. These papers mention channel modeling for UAVs in various environments, which can be evaluated with high accuracy by analyzing them through rigorous channel modeling [33–35]. Research on channel modeling for operating UAVs is also in progress. The simulator developed in this study is a simplified channel modeling that only implements geometry such as buildings. In the future, when more detailed analysis becomes necessary, we plan to perform detailed modeling of the propagation environment, taking into account scenarios, parameters, shadows, etc.

2.2. Conventional Methods and Issues

Related studies have not adequately discussed the problems associated with handovers, such as the communication environment with the connection destination based on the location where the drone has moved and the conditions for switching the connection destination. In other words, it is important to devise a handover method that is suitable for drones because drones move faster than conventional handovers on the ground, which assume tablets and cellular terminals. In addition, handover technology to switch connection destinations while drones are flying has not yet been studied. In conventional handover, if handover is performed using only simple received power, the received power will be determined to be high, including the interference power due to multipath, so it is difficult to select the optimal handover trigger and the optimal AP. Therefore, multipath interference due to building reflections and diffraction is not included. The handover is performed when the received power from the base station to which the drone is connected decreases, as shown in Figure 6, but the signal is reflected by multipath due to buildings and other factors, resulting in interference waves. Even if the power received from the AP is high, SINR becomes low and communication quality deteriorates. Therefore, it is necessary to make a handover decision by considering the SINR, which changes continuously based on the flight, rather than simply checking the received power. Based on these considerations, it is also necessary to include the requirement for drones to fly in environments that include buildings, etc. It is necessary to construct a new evaluation method that includes multipath interference in 3D space and time series by flight, which is different from the conventional evaluation method for ground communication.

The conventional connection switchover trigger in a handover uses the sequence shown in Figure 7 if the authentication procedure is omitted. If the STA, which is a mobile station, continuously receives beacons, it recognizes that it is in the communication area under the AP and maintains the connection. When the beacon signal cannot be received an arbitrary number of times, the STA decides to perform a handover and connects to a new AP based on the information of a beacon signal with high reception power that has been searched for in advance. In the conventional method, a handover is not performed even if the received power is low, unless the beacon signal is not received. In other words, even if the signal from the current AP weakens and the communication speed decreases, a connection cannot be established with an AP with better conditions. One of the objectives of this study is to solve these problems.

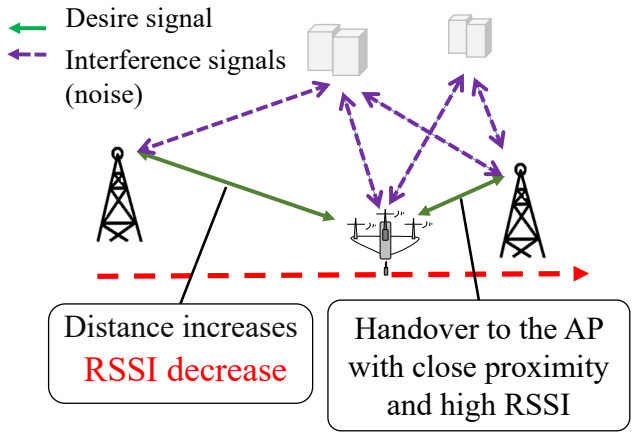

Figure 6. Handover and multipath interference from drone flight.

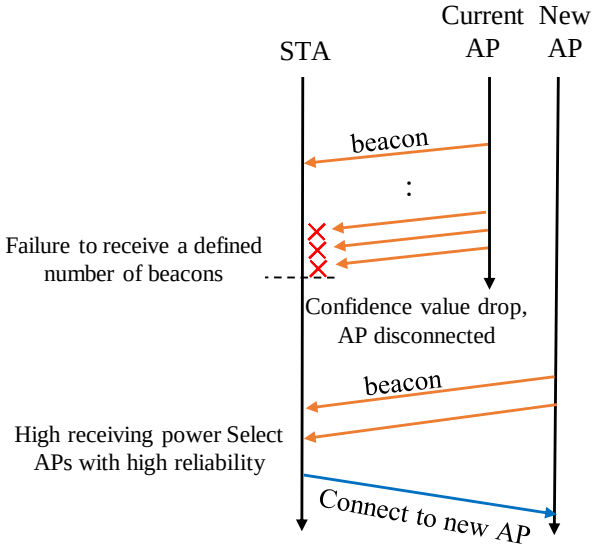

Figure 7. Conventional handover sequence.

3. How to Evaluate Flying Drones

A wireless network evaluation is typically performed layer-by-layer. Examples include antenna characteristics, propagation characteristics, network protocols, and the application quality of service. However, because drones can construct a three-dimensional network in the air, buildings and obstacles in urban areas can reflect and block the network, resulting in multipath interference. Unlike conventional methods for evaluating terrestrial networks, propagation conditions are highly complex and depend on the height of buildings, the drone's flight altitude, and the speed of movement of the drone. In addition, these propagation conditions have a significant impact on upper-layer communication protocols. In other words, the actual applications and quality of service also vary. Therefore, if a service operation is to be launched, it is necessary to conduct an evaluation and verification in a real environment; however, conducting experiments using actual flying drones is a significant hurdle. Moreover, apart from drone communications, ground station services also require significant operation time and cost for propagation experiments during station design. Propagation characteristics such as SINR and bit error rate (BER) of the physical layer have been used as evaluation indices for wireless communications. However, because the wireless communication services used by users include upper-layer protocol performance, such as streaming and net surfing, it is necessary to evaluate the communication quality of user-based applications. In addition to the difficulty in the analysis methods and evaluation indices that integrate the various layer technologies, the simultaneous analysis of signal processing at the physical layer and the analysis of radio propagation has resulted in sim-

plified and inaccurate evaluation results [36]. In this study, we developed and evaluated a cross-layer computer simulator, from the physical layer to the internet protocol (IP) layer. This simulator is characterized by its ability to evaluate the impact of multipath interference caused by structures on throughput at the (IP) layer, such as the transmission control protocol (TCP) and user data gram protocol (UDP). Moreover, it can evaluate time-series data assuming a high-speed drone flight. The advantage of the simulator is that even engineers without expertise in the physical or higher layers can easily evaluate the performance of the entire system, regardless of where the service is provided. In other words, apart from drone networks, new communication methods devised in the future will be in great demand for virtual evaluation prior to the development of actual equipment.

3.1. Overview of 3D Cross Layer Simulator

In this study, a three-dimensional cross-layer simulator was developed for the virtual evaluation of drone flight. The simulator configuration is shown in Figure 8. The simulator uses a physical propagation simulator (EEM: ray tracing method) and numerical analysis software (MATLAB R2020a: OFDM signal processing) [37] for the physical layer, and a network simulator (OPNET: including network protocol, and the upper layer uses a network simulator (OPNET: including network protocols and applications) [38]. A control tool that optimally transfers information data between these commercially available analysis simulators was constructed, which passes the received power analyzed at the physical layer to a network simulator at a higher layer for continuous and integrated evaluation from the physical layer to the application layer. In addition, topography and building data are imported from the map data, thereby enabling analysis in a virtual network environment with a 3D configuration. Furthermore, the system can handle the performance evaluation of the entire system as well as the evaluation indices and extracted analysis specified for each layer. The ray tracing method converts radio waves into optical waves. The ray tracing method approximates radio waves as light using direct waves and reflection and diffraction paths and enables analysis, including real-space conditions, for performance evaluation between transmitting and receiving stations using drones and other devices with height differences. Figure 9 shows the structure of the linkage of each simulator, which exchanges propagation information and signal processing analysis information between the EEM and MATLAB. The results of these analyses were passed to OPNET, which uses network protocols to evaluate the throughput and delay. As the drone (STA) flies and moves, the results of each propagation and signal analysis are output as a CSV file and fed back into the OPNET evaluation model. However, the number of output CSV files increases as time is divided based on the moving speed and the desired analysis accuracy. Therefore, it is necessary to divide the time into an appropriate number of analyses. The simulation flow divides the drone flight path into arbitrary time segments, as shown in Figure 10, and performs a propagation analysis for each point at each segmented time. The transmission rate is determined by selecting the modulation and coding scheme index (MCS index) that can be transmitted based on the received power obtained from the propagation analysis. The result of the determined transmission rate is passed to the upper layer to calculate the throughput. The throughput is calculated at the Layer 2 level, including the media access control (MAC) header and control frame transmission and reception procedures, as well as the throughput available to the application, including the frame header and control frame transmission and reception procedures above the IP layer. Moreover, it supports traffic such as video, voice, hypertext transfer protocol (HTTP), and evaluation metrics for each layer, facilitating the performance evaluation of applications.

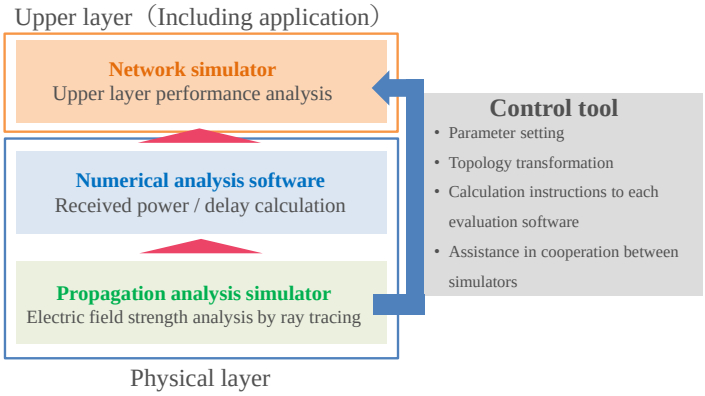

Figure 8. Three-dimensional cross layer simulator configuration.

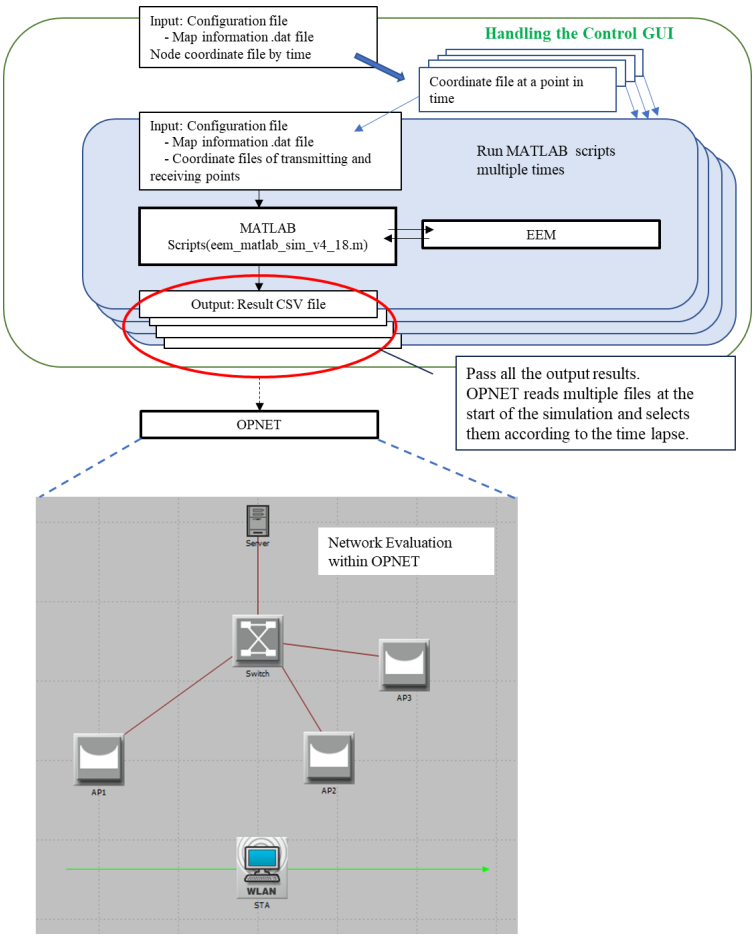

Figure 9. Simulator linkage.

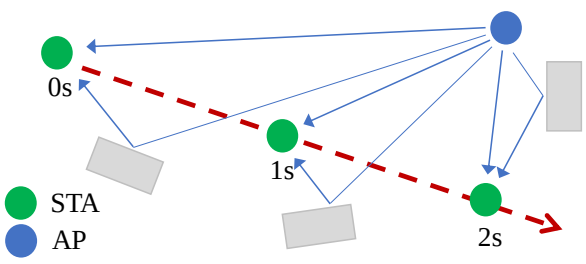

Divide into intervals of 1s , 5km/h

Figure 10. Simulation flow.

3.2. Power Calculation Method in 3D Cross Layer Simulator

The calculation of the received power and SINR in the simulator follows the procedure shown in Figure 11 and Equation (1), which are explained below. The simulator incorporated a ray-tracing method that considers radio waves as rays. Map data containing terrain and buildings were prepared, and multiple rays from connected APs, other APs, and STAs were analyzed using the propagation analysis simulator. The received power P_r [dBW] was calculated from the analyzed ray and converted to the true unit of received power $\overline{P}_r$ [mW] using Equation (1).

$$\overline{P}_r = \sum_{i=1}^{N} 10^{\frac{P_r^{(i)}}{10}} \times 10^3, \tag{1}$$

where $P_r^{(i)}$ denotes the received power of the ith ray and N denotes the maximum number of rays.

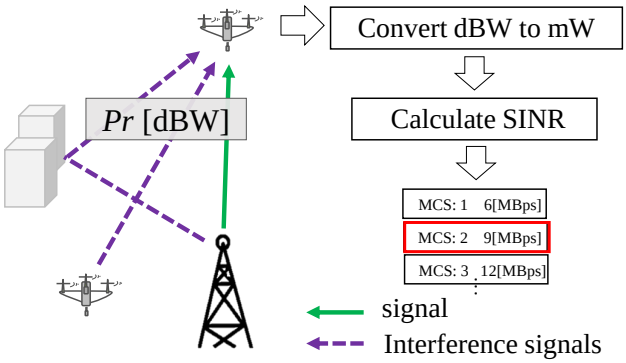

Figure 11. Flow of SINR calculation.

Subsequently, SINR is calculated from Equation (2) using the maximum value of the converted received power, interference power, and interference power from other APs, and a table corresponding to SINR for the signals from each AP a is created.

$$\mathrm{SINR} = \frac{P_r}{\sigma + \max_{n \in \mathcal{A} \setminus \{a\}} P_n}, \tag{2}$$

where σ denotes the interference power beyond the GI (guard interval) length plus the thermal noise, $\mathcal{A}$ denotes the set of access points, and P_n denotes the interference power from access point $n \in \mathcal{A} \setminus \{a\}$. GI is the signal interval used to avoid inter-symbol interference (ISI) of delayed waves in a multipath environment. In this study, the length of GI was set to 800 ns. To obtain the transmission rate from the obtained SINR, the minimum receiving sensitivity $R_{\min}$ [dB] was calculated using Equation (3), and the corresponding MCS was selected, as shown in Figure 11.

$$R_{\min} = \mathrm{SINR} - 85 \tag{3}$$

Because the interference power was analyzed using the simulator, a guard interval function was added to improve the multipath interference, as specified in the IEEE802.11ax standard [39]. As shown in Equation (4), if the multipath delay time t is shorter than the guard interval length GI, the signal is considered a valid signal.

$$t \leqq \mathrm{GI} \tag{4}$$

Conversely, if the delay time is longer than the guard interval length, as shown in Equation (5), the signal is considered an interference.

$$t \geqq \mathrm{GI} \tag{5}$$

However, in this developed simulator, simple channel modeling was used, which only implements the geometry of buildings and other structures. Analysis in rigorous channel modeling for air–ground requires consideration of buildings and their materials and dielectric constants [31,32]. In future work, modeling of the propagation environment will be implemented when more detailed analysis is required.

Further discussing the simulator developed, the only uncertainty is the movement of the drone. In order to reproduce a dynamic propagation environment, other objects are assumed to move, and for evaluations that assume a vehicle, such as the V2X communication presented in reference [40], it is necessary to implement a Monte Carlo-like method for vehicle movement. The developed simulator is an event-driven method. This simulation method is that the analysis will be complex and require high computer specifications. In addition, because the system is event-driven, it is difficult to perform statistical evaluations such as numerical analysis. However, it can be extended to general cases, such as implementing propagation environment changes in a time series or setting parameters for arbitrary channel estimation errors. Therefore, although the method is not suitable for statistical evaluation, it is suitable for propagation model evaluation for social implementation and performance evaluation of new communication systems, which are the goals of this study, and we expect that it will contribute to similar research.

3.3. Evaluation Results of Conventional Methods

The developed simulator was used to evaluate a conventional handover sequence, as shown in Figure 7. The simulation model of the conventional method was evaluated using STA flight paths on the map shown in Figure 12. The map was obtained using the GSI map data download service [41]. In this map, the drone at the mobile station is designated as an STA and repeats the handover while passing along the red-dotted path from AP1 to AP4 of the base station. The service model assumes that the STA uploads video images captured while flying to the AP on the ground and continuously sends UDP data from the STA to the AP.

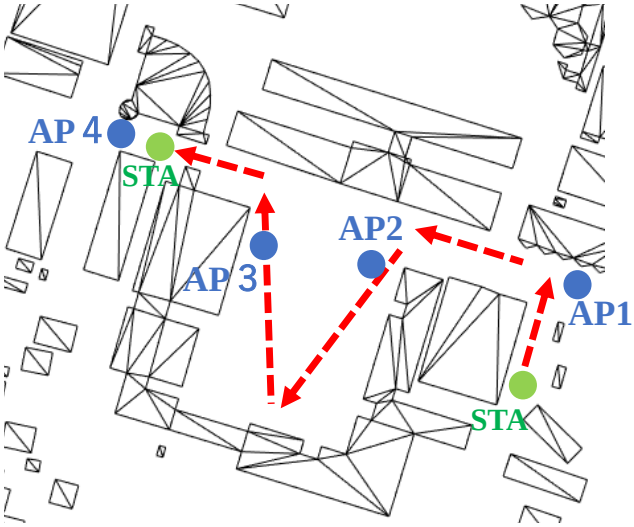

Figure 12. Simulation model and flight path.

Table 1 lists the parameters used for the evaluation. The communication method used was the IEEE802.11g standard [42], frequency band 2.4 GHz, and transmission power 0.2 mW. The STA and AP were at the same height of 5 m above the ground, and the flight speed of the STA was 5 km/h.

The simulation results for the evaluation model are presented in Figure 13. Figure 13 shows time [s] on the horizontal axis and throughput [Mbps] on the vertical axis. Handover occurs between AP1 and AP4; however, after connecting to AP2, a period of low throughput is followed by a connection to AP4 without connecting to AP3 because no beacon reception

failure occurs after handover to AP2; therefore, the decision to initiate handover is not made, and the connection to AP2 with low reception power is maintained, resulting in a situation where handover to AP3 with high reception power cannot be performed. These results confirm that the handover to the optimal AP is not performed unless a beacon failure occurs in the conventional method.

Table 1. Evaluation parameters.

	Conv. Method
Comn. method	IEEE802.11g standard
Frequency band	2.4 GHz
Transmission power	0.2 mW
Flight speed	5 km/h
STA and AP height	5 m above ground
Hand over method	Beacon reception failure counts

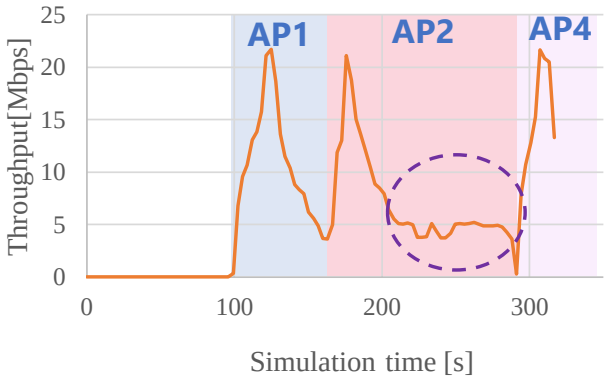

Figure 13. Evaluation results of conventional methods.

4. Proposal Method According to the Issue

In this section, we propose two methods to solve these problems and demonstrate their effectiveness through simulation evaluation.

Proposed method #1: In the conventional method, a handover to a better-conditioned base station cannot be performed unless a beacon failure occurs. In proposed method #1, the handover decision is based on a SINR threshold instead of beacon reception. The proposed method solves this problem by actively performing handovers from an AP with a low transmission rate to another AP with good conditions.

Proposed method #2: Since proposed method #1 performs handover aggressively, if a connection is attempted with a base station whose reception power is momentarily high due to the influence of buildings, etc., the reception power drops immediately and handover is performed again immediately, which increases the number of handover attempts. To solve this problem, the number of handover attempts can be reduced by eliminating base stations with instantaneously high received power from handover candidates by acquiring a moving average with reference to the past received power.

4.1. Overview of Proposed Method #1

As described in Section 2.2, the conventional handover method cannot perform a handover to a base station with good conditions unless a beacon failure occurs, even in an environment where SINR is low and communication conditions are poor, and the connection to a base station with a low transmission speed continues. Method #1 proposes a connection destination selection method that operates based not only on the availability of beacon reception but also on handover timing and the MCS index with SINR as a threshold

for optimal connection destination switching. Using the SINR as the threshold value, even if a connection to a base station with a low SINR continues without beacon reception failure, as shown in Figure 13 in the conventional method, a handover decision can be made, and the AP can proactively connect to an AP with better conditions.

Figure 14 shows the handover procedure for proposed method #1. As a specific procedure in the proposed method, the STA first sets the SINR threshold before the system is operated. At the beginning of the system operation, the STA sets the SINR threshold for a certain period after receiving a beacon. If the SINR threshold is exceeded, the STA recognizes that it is in the communication area under the AP and maintains the connection. When the SINR of the AP to which the drone is connected drops below the threshold value due to the drone's movement, the system decides to perform a handover and determines the MCS index of each AP based on the beacon searched for in advance. The AP to be connected next is then determined.

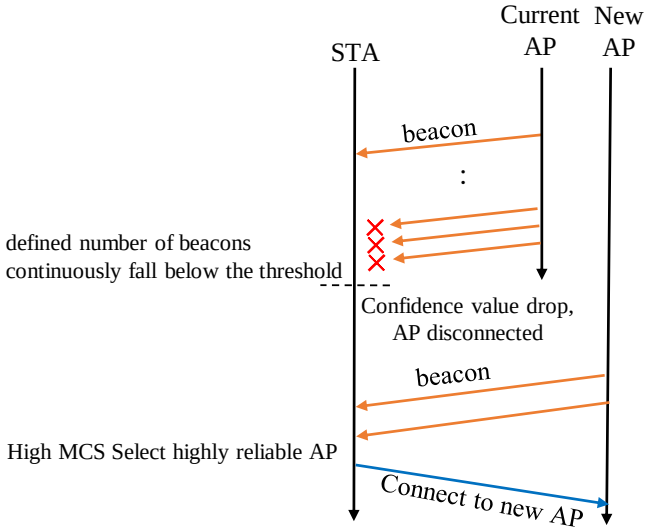

Figure 14. Handover sequence of proposed method #1.

The algorithm for AP selection is as follows:

if (MCS index $\geq$ 1, AP exists)
Handover to the AP with the best SINR among the applicable APs.

else if (MCS index $\geq$ 1, AP does not exist)
Handover to the AP with the best SINR among the APs with the same MCS index as the current one.

SINR threshold compares the SINR value calculated from the beacon to the value set for the AP-switching threshold. In this study, SINR was set to 6 dB to guarantee the minimum transmission rate. Using this method, a handover to a base station with better conditions is performed even when the received power of the beacon signal is low.

The flowchart of proposed method #1 is shown in Figure 15. In proposed method #1, SINR is calculated when a beacon is received and the data table of SINR is updated. It then compares the SINR threshold value with the calculated SINR value, and it disconnects from the AP if the SINR value falls below the threshold.

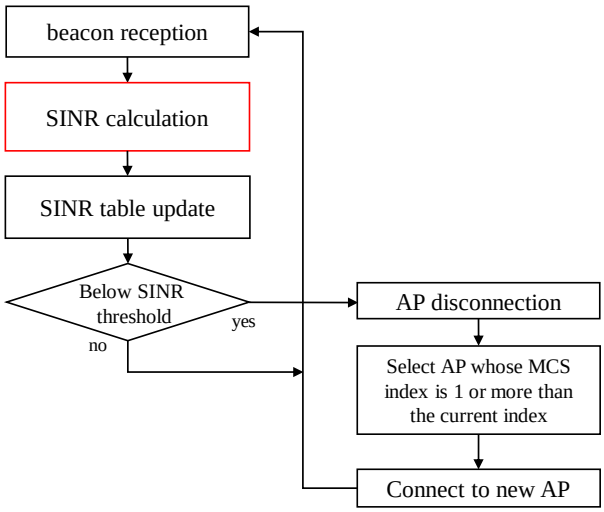

Figure 15. Flowchart of proposed method #1.

4.2. Evaluation Method and Results of Proposed Method #1

To compare the conventional method and proposed method #1, we evaluated the parameters as indicated in Table 2, where the communication method is the IEEE802.11g standard, frequency band is 2.4 GHz, transmission power is 0.2 mW, and drone speed is 5 km/h.

Table 2. Parameters for evaluation comparison.

	Conv. Method	**Prop. #1**	**Prop. #2**
Communication method	IEEE802.11g standard		
Frequency band	2.4 GHz		
Transmission power	0.2 mW		
Flight speed	5 km/h		
Hand over method	Beacon counts	SINR threshold	SINR moving average

Proposed method #1 uses the same simulation model as that shown in Figure 12, which is used in the evaluation of the previous method. The STA repeatedly handovers from AP1 to AP4, passes through the red-dotted path, and continuously uploads UDP data from the STA. Figure 16 compares the throughput characteristics of the conventional and proposed (#1) methods. The horizontal axis represents the time [s], and the vertical axis represents the throughput [Mbps]. In the conventional method, periods of low throughput exist because the handover is performed from AP2 to AP4 without connecting to AP3, as previously described. This is because, when the STA is connected to AP1 and AP2, it performs a handover before the connection link is disconnected due to the absence of other base stations with high reception strength in the vicinity. However, when the STA heads to AP3, the connection to AP2 is not made, the connection to AP3 is not made, and a handover is not performed until AP4, where AP2 is disconnected. This not only reduces the throughput, but also causes the connection to drop before 300 s. In contrast, proposed method #1 performs optimal AP selection by referring to the SINR threshold and MCS index, independent of whether a beacon is received. In other words, it performs a handover to AP3 even when the AP2 beacon is received. Compared with the conventional method, the proposed method achieves a maximum throughput of 20 Mbps or higher in the communication area of AP3, and the handover is performed seamlessly without loss of connection when switching to AP4. These results confirm the effectiveness of proposed method #1, SINR threshold, for an optimal handover.

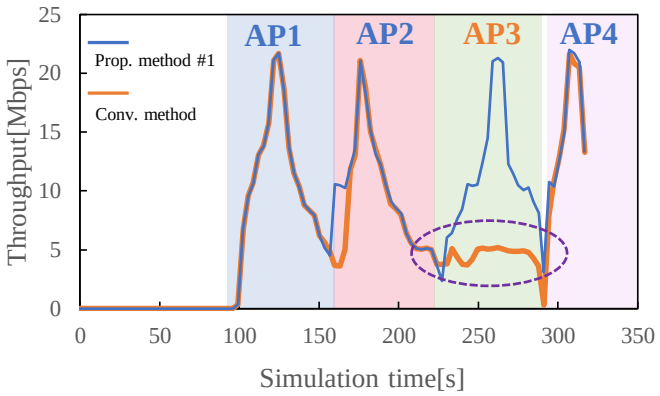

Figure 16. Evaluation results of proposed method #1.

4.3. Overview of Proposed Method #2

Handover using proposed method #1 was confirmed to be effective in reducing the time of communication disconnection and the low transmission rate by performing a handover to the optimal AP by following the SINR threshold before the beacon signal is completely disconnected. However, if, for example, an AP on the flight path is locally shielded by a building and cannot receive a high signal until just before it passes, it may perform an unnecessary handover with a very short connection period and may not achieve a stable communication speed. A topographic map of the area is shown in Figure 17 assuming such an environment. This condition is the simulation model of a localized area, as shown in Figure 12. The STA is assumed to fly along a straight path, and the location of AP2, which exists in the vicinity of AP1 to AP3, is subject to a low received power until the STA passes immediately in front of it, due to the surrounding shielding. The STA moves further and obtains high received power from AP2, but immediately after passing AP2, the received power drops again. Using proposed method #1 in such an environment, the connection to AP2, which has a locally high SINR, is immediately disconnected, requiring a handover to another AP, which increases the overhead caused by the switching time connecting to the destination. To solve this problem, proposed method #2 uses the moving average value calculated based on the past SINR values during the flight as a decision index for handover to prevent connection to an AP with a locally high SINR.

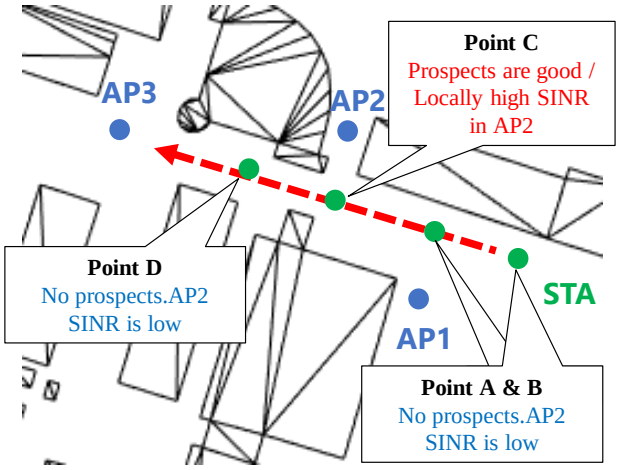

Figure 17. Environmental conditions with frequent handovers.

Figure 18 shows the handover procedure for proposed method #2. Proposed method #1 implements the aforementioned handover timing based on SINR as a threshold and a destination selection method that operates based on the MCS index. On the other hand,

proposed method #2 measures SINR before and calculates the moving average using the latest SINR and statistics referring to the past SINR by Equation (6). Using the proposed method, SINR can be estimated by referring to past values when measuring SINR, such that the locally high SINR can be estimated to be low.

$$\text{Moving Average} = \frac{1}{M}\sum_{i=1}^{M} S_i, \tag{6}$$

where S_i indicates SINR at each point by assigning a number i to each point along the divided travel route, and M denotes the total number of points referred to in the past. Using the proposed method, the locally high SINR can be estimated as low because past values can be referred to when measuring SINR.

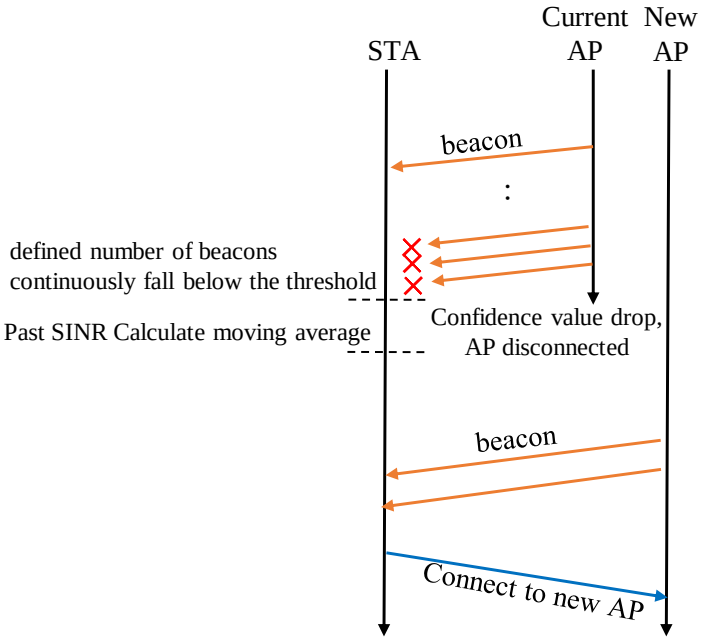

Figure 18. Handover sequence for proposed method #2.

The flowchart of proposed method #2 is shown in Figure 19. In proposed method #2, in addition to the procedure of proposed method #1, after calculating the SINR, the moving average value of the SINR is calculated by referring to the past SINRs. This moving average is compared with the threshold value to make a handover decision.

An example of the operation of proposed method #2 is illustrated using an example image of the SINR values obtained from each AP in Table 3 and the terrain configuration in Figure 17. In Figure 17, the STA handovers APs from points A to D while flying over the green points. Point C refers to the point at which a high SINR value is obtained from AP2. Table 3 shows the moving average of SINR for points A to D and the SINR for point C. For the case of proposed method #1, which refers only to the SINR of each point in the topography of Figure 17, moving to point C connects to AP2 whose SINR in Table 3 is 30 dB at the highest value. However, by moving to point D, the SINR of AP2 decreases and is immediately connected to that of AP3, which has a higher SINR. In such an environment, where APs with high SINR exist locally, handovers occur frequently, making it difficult to maintain seamless communication.

Therefore, proposed method #2 calculates the moving average of SINR at each point and prevents SINR from suddenly becoming high at a certain point. As an example, in Table 3, at point C, AP2 has the highest SINR at 30 dB; however, the moving average at point C (Ave.) is calculated by referring to past values at each AP. The calculated moving averages are 9 dB for AP1, 16.5 dB for AP2, and 21 dB for AP3. Based on these results, proposed method #2 can prevent unnecessary handovers by selecting AP3 instead of AP2.

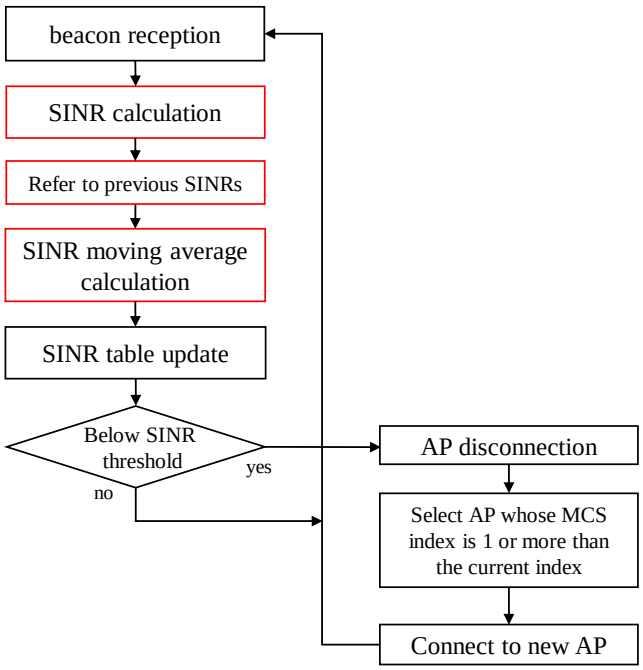

Figure 19. Flowchart of proposed method #2.

Table 3. Example of moving average [dB] of acquired SINR in flight movement.

Point	AP1	AP2	AP3
A	28	0	0
B	15	3	14
C	3	**30**	28
C (Ave.)	9	16.5	**21**
D	0	3	30

4.4. Evaluation Method and Results of Proposed Method #2

Proposed method #2 selects the best AP for handover based on the moving average of SINR. However, when the drone's flight speed is high, proposed method #2 is unnecessary in some cases because the drone is connected to the next AP before finding the AP with a locally high SINR. Therefore, to confirm the effect of the proposed method on the speed of flight of the STA, we compared the average throughput when using proposed methods #1 and #2 on the map shown in Figure 17. The flight speed of the STA was varied from 20 to 50 km/h in increments of 10 km/h. The STA continues to upload the UDP data while performing a handover via the green point in Figure 17. The simulation parameters are listed in Table 2. To monitor the behavior of handover to APs with locally higher SINR, the evaluation method was based on the average throughput extracted from the portion of Figure 20 where the drone passes in the vicinity of AP2. The results of the average throughput for flight speeds comparing proposed methods #1 and #2 are shown in Figure 21. Proposed method #2 had a higher average throughput than proposed method #1 at flight speeds of 30 and 40 km/h. In particular, at a flight speed of 40 km/h, the proposed method #2 has a higher average throughput than proposed method #1. In particular, at a flight speed of 40 km/h, the average throughput of proposed method #2 was approximately 48% higher than that of proposed method #1. On the other hand, at a slower flight speed of 20 km/h, both proposed methods #1 and #2 handover to AP2 and stay connected to AP2 for a long time; therefore, proposed method #2 is ineffective. In addition, when the flight speed is 50 km/h, both proposed methods #1 and #2 pass through AP2 at high speed, and no

handover is performed; therefore, proposed method #2 is also not effective. These results confirm that proposed method #2 is effective at flight speeds between 30 and 40 km/h.

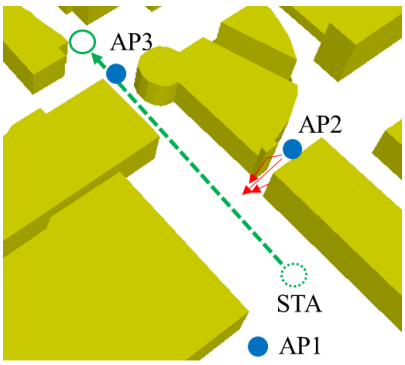

Figure 20. Maps for evaluation of proposed method #2.

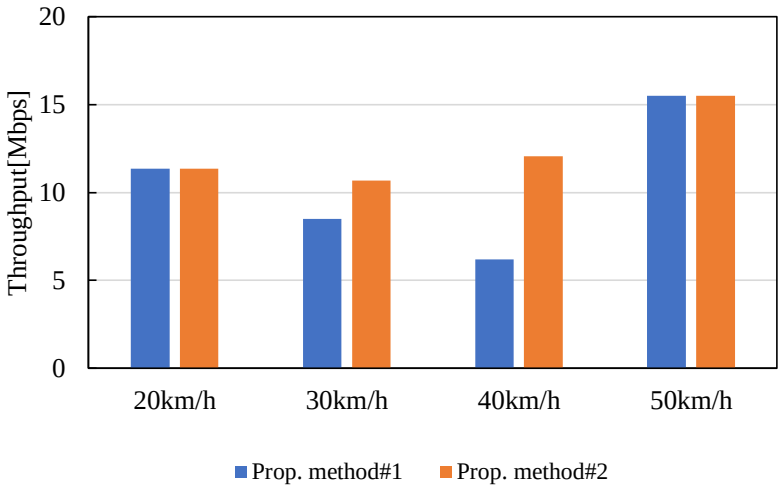

Figure 21. Average throughput of proposed methods #1 and #2 with respect to flight speed.

For a detailed evaluation of proposed method #2, we compared its throughput with that of proposed method #1 using the map in Figure 17. Figure 22 shows the throughput characteristics at a flight speed of 40 km/h; the best result is shown in Figure 21. When using proposed method #1, the STA is initially connected to AP1, and, as it moves, the SINR of AP1 decreases. When it moves closer to AP2, it establishes a connection with AP2, which has a higher SINR. However, after connecting to AP2, the SINR threshold of AP2 is immediately lowered and the connection is immediately converted to AP3. When an AP with a locally high SINR exists, the handover is repeated multiple times each time, resulting in a decrease in throughput. On the other hand, proposed method #2, searches for the next AP when the SINR of AP1 becomes lower than the threshold value. When moving near AP2, even though SINR increases rapidly, SINR is estimated to be low when calculating the moving average because of the low SINR of AP2 in the past. Therefore, AP2 was removed from the candidate handover destinations, and AP3 was selected as the next connection destination. By reducing the number of handover attempts in this manner, the throughput degradation was also reduced, and it was confirmed that the throughput was maintained on average.

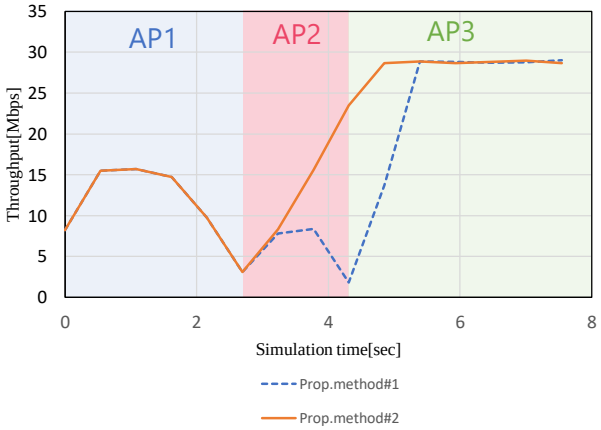

Figure 22. Comparison results of proposed methods #1 and #2 at a flight speed of 40 km/h.

5. Conclusions

Relay transmission using drones as radio stations enables flexible network construction in air through handovers with ground stations. However, the presence of structures or obstacles in the flight path causes multipath interference, and the propagation environment fluctuates significantly during flight. In such a communication environment, it is difficult for a drone to select an optimal ground station for a handover. Additionally, unlike a terrestrial network, the propagation environment of a flying drone is affected by structures and other factors that cause multipath interference based on the flight speed and altitude, making the propagation environment conditions even more complex.

To solve these problems, we proposed handover schemes between drones and the ground that consider multipath interference caused by obstacles. Proposed method #1 performs optimal handover considering interference by setting a SINR threshold when searching for surrounding APs, and we confirmed that the proposed method can achieve a maximum throughput of 20 Mbps or higher when the conventional method achieves a throughput of 5 Mbps or lower. Proposed method #2 avoids unnecessary handovers based on travel speed, and the average throughput is improved by a maximum of approximately 48%. The evaluation results demonstrate the effectiveness of the two proposed methods and the realization of a seamless handover.

For the actual operation of the proposed method, in proposed method #1, the drone collects beacon signals of each traced radio pass while moving outdoors and performs handover according to the SINR threshold value. At the same time, using proposed method #2, the moving average is calculated by using statistics collected from SINR in environments where SINR tends to be frequently high locally, such as urban areas. Handover is performed to the AP with the highest SINR calculated from the moving average. The drone flight speed at which proposed method #2 is effective is 30–40 km/h, which is a medium speed.

Author Contributions: Conceptualization, T.H., T.M. and S.U.; method, T.H., T.M., T.I. and J.H.; validation, K.H. and T.H.; investigation, K.H., T.K. and K.M.; resources, K.H.; data curation, K.H.; writing—original draft preparation, K.H., T.H. and T.K.; writing—review and editing, T.H., T.K. and K.M.; visualization, K.H.; supervision, T.M., T.I., J.H. and K.M.; project administration, T.H. and S.U.; funding acquisition, T.H., T.M., T.I. and J.H. All authors have read and agreed to the published version of the manuscript.

Funding: This research was supported by SCOPE (JP215004001) of the Ministry of Internal Affairs and Communications.

Data Availability Statement: Data are available from the authors upon request.

Conflicts of Interest: The authors declare no conflicts of interest.

References

1. 3rd Generation Partnership Project. TS 23.501: Technical Specification Group Services and System Aspects; System Architecture for the 5G System; Stage 2 (Release 16). 3GPP. July 2020. Available online: https://portal.3gpp.org/desktopmodules/Specifications/SpecificationDetails.aspx?specificationId=3493 (accessed on 8 December 2023).
2. Qi, W.; Wang, H.; Xia, X.; Mei, C.; Liu, Y.; Xing, Y. Research on Novel Type of Non Terrestrial Network Architecture for 6G. In Proceedings of the 2023 International Wireless Communications and Mobile Computing (IWCMC), Marrakesh, Morocco, 19–23 June 2023; pp. 1281–1285. [CrossRef]
3. Kafle, V.P.; Sekiguchi, M.; Asaeda, H.; Harai, H. Integrated Network Control Architecture for Terrestrial and Non-Terrestrial Network Convergence in Beyond 5G Systems. In Proceedings of the 2022 ITU Kaleidoscope-Extended Reality—How to Boost Quality of Experience and Interoperability, Accra, Ghana, 7–9 December 2022; pp. 1–9. [CrossRef]
4. Yue, Y.; Tang, X.; Yang, W.; Zhang, X.; Zhang, Z.; Gao, C.; Xu, L. Delay-aware and Resource-efficient VNF placement in 6G Non-Terrestrial Networks. In Proceedings of the 2023 IEEE Wireless Communications and Networking Conference (WCNC), Glasgow, UK, 26–29 March 2023; pp. 1–6. [CrossRef]
5. Sattarzadeh, A.; Liu, Y.; Mohamed, A.; Song, R.; Xiao, P.; Song, Z.; Zhang, H.; Tafazolli, R.; Niu, C. Satellite-Based Non-Terrestrial Networks in 5G: Insights and Challenges. *IEEE Access* **2022**, *10*, 11274–11283. [CrossRef]
6. Majamaa, M.; Martikainen, H.; Sormunen, L.; Puttonen, J. Adaptive Multi-Connectivity Activation for Throughput Enhancement in 5G and Beyond Non-Terrestrial Networks. In Proceedings of the 2022 International Conference on Software, Telecommunications and Computer Networks (SoftCOM), Split, Croatia, 22–24 September 2022; pp. 1–5. [CrossRef]
7. Evans, B. 6G Satellite Communications. In Proceedings of the 2022 27th Asia Pacific Conference on Communications (APCC), Jeju Island, Republic of Korea, 19–21 October 2022; pp. 175–177. [CrossRef]
8. Kawanishi, T. Seamless Networks for beyond 5G. *IEEE Future Netw. Tech Focus* **2019**, *3*.
9. Cassiau, N.; Kim, I.; Strinati, E.C.; Noh, G.; Pietrabissa, A.; Arnal, F.; Casati, G.; Choi, T.; Choi, Y.J.; Chung, H.; et al. 5G-ALLSTAR: Beyond 5G Satellite-Terrestrial Multi-Connectivity. In Proceedings of the 2022 Joint European Conference on Networks and Communications & 6G Summit (EuCNC/6G Summit), Grenoble, France, 7–10 June 2022; pp. 148–153. [CrossRef]
10. Shayea, I.; Ergen, M.; Azmi, M.H.; Çolak, S.A.; Nordin, R.; Daradkeh, Y.I. Key Challenges, Drivers and Solutions for Mobility Management in 5G Networks: A Survey. *IEEE Access* **2020**, *8*, 172534–172552. [CrossRef]
11. Lei, L.; Yuan, Y.; Vu, T.X.; Chatzinotas, S.; Minardi, M.; Montoya, J.F.M. Dynamic-Adaptive AI Solutions for Network Slicing Management in Satellite-Integrated B5G Systems. *IEEE Netw.* **2021**, *35*, 91–97. [CrossRef]
12. Ozger, M.; Godor, I.; Nordlow, A.; Heyn, T.; Pandi, S.; Peterson, I.; Viseras, A.; Holis, J.; Raffelsberger, C.; Kercek, A.; et al. 6G for Connected Sky: A Vision for Integrating Terrestrial and Non-Terrestrial Networks. In Proceedings of the 2023 Joint European Conference on Networks and Communications & 6G Summit (EuCNC/6G Summit), Gothenburg, Sweden, 6–9 June 2023; pp. 711–716. [CrossRef]
13. Available online: https://www.soumu.go.jp/johotsusintokei/whitepaper/ja/r05/html/nd242330.html (accessed on 8 December 2023).
14. Li, S.; Chen, Q.; Meng, W.; Li, C. Civil Aircraft Assisted Space-Air-Ground Integrated Networks: An Innovative NTN of 5G and Beyond. *IEEE Wirel. Commun.* **2022**, *29*, 64–71. [CrossRef]
15. Harounabadi, M.; Heyn, T. Toward Integration of 6G-NTN to Terrestrial Mobile Networks: Research and Standardization Aspects. *IEEE Wirel. Commun.* **2023**, *30*, 20–26. [CrossRef]
16. Cui, H.; Zhang, J.; Geng, Y.; Xiao, Z.; Sun, T.; Zhang, N.; Liu, J.; Wu, Q.; Cao, X. Space-air-ground integrated network (SAGIN) for 6G: Requirements, architecture and challenges. *China Commun.* **2022**, *19*, 90–108. [CrossRef]
17. Dureppagari, H.K.; Saha, C.; Dhillon, H.S.; Buehrer, R.M. NTN-Based 6G Localization: Vision, Role of LEOs, and Open Problems. *IEEE Wirel. Commun.* **2023**, *30*, 44–51. [CrossRef]
18. Azari, M.M.; Solanki, S.; Chatzinotas, S.; Kodheli, O.; Sallouha, H.; Colpaert, A.; Montoya, J.F.M.; Pollin, S.; Haqiqatnejad, A.; Mostaani, A.; et al. Evolution of Non-Terrestrial Networks From 5G to 6G: A Survey. *IEEE Commun. Surv. Tutorials* **2022**, *24*, 2633–2672. [CrossRef]
19. Gu, X.; Zhang, G. A survey on UAV-assisted wireless communications: Recent advances and future trends. *Comput. Commun.* **2023**, *208*, 44–78. [CrossRef]
20. Li, B.; Zhao, S.; Miao, R.; Zhang, R. A survey on unmanned aerial vehicle relaying networks. *IET Commun.* **2021**, *15*, 1262–1272. [CrossRef]
21. Available online: https://www.docomo.ne.jp/info/news_release/2022/02/09_00.html (accessed on 8 December 2023).
22. *Open Systems Interconnection—Basic Reference Model*; International Organization for Standardization ISO: Geneva, Switzerland, 1984.
23. *IEEE 802.11-1997*; Information Technology—Telecommunications and Information Exchange between Systems—Local and Metropolitan Area Networks—Specific Requirements—Part 11: Wireless LAN Medium Access Control (MAC) and Physical Layer (PHY) Specifications. IEEE: Piscataway, NJ, USA, 1997.
24. *IEEE Std 802.11r-2008*; Amendment 2: Fast BSS Transition. IEEE: Piscataway, NJ, USA, 2008.

25. Chou, F.-Y.; Liao, I.-J.; Li, Y.-C.; Wu, T.-Y.; Lee, W.-T. A Pre-registered Handoff Scheme in IEEE 802.11r Wireless Local Area Networks. In Proceedings of the 2010 International Conference on Communications and Mobile Computing, Shenzhen, China, 12–14 April 2010; pp. 466–470. [CrossRef]
26. *IEEE Std 802.11r-2008* ; IEEE Standard for Information Technology—Local and Metropolitan Area Networks—Specific Requirements—Part 11: Wireless LAN Medium Access Control (MAC) and Physical Layer (PHY) Specifications Amendment 2: Fast Basic Service Set (BSS) Transition. Amendment to IEEE Std 802.11-2007 as Amended by IEEE Std 802.11k-2008. IEEE: Piscataway, NJ, USA, 2008; pp.1–126. https://doi.org/10.1109/IEEESTD.2008.4573292.
27. Clancy, T.C. Secure handover in enterprise WLANs: Capwap, hokey, and IEEE 802.11R. *IEEE Wirel. Commun.* **2008**, *15*, 80–85. [CrossRef]
28. Hiraguri, T.; Nishimori, K.; Shitara, I.; Mitsui, T.; Shindo, T.; Kimura, T.; Matsuda, T.; Yoshino, H. A Cooperative Transmission Scheme in Drone-Based Networks. *IEEE Trans. Veh. Technol.* **2020**, *69*, 2905–2914. [CrossRef]
29. Matsumura, N.; Nishimori, K.; Taniguchi, R.; Mitsui, T.; Hiraguri, T. Effect of Propagation Environment Control Method Using Drone MIMO Relay Station. In Proceedings of the 2018 International Symposium on Antennas and Propagation (ISAP), Busan, Republic of Korea, 23–26 October 2018; pp. 1–2.
30. Wang, X.; Mi, Z.; Wang, H.; Zhao, N. Performance test and analysis of multi-hop network based on UAV Ad Hoc network experiment. In Proceedings of the 2017 9th International Conference on Wireless Communications and Signal Processing (WCSP), Nanjing, China, 11–13 October 2017; pp. 1–6. [CrossRef]
31. Khuwaja, A.A.; Chen, Y.; Zhao, N.; Alouini, M.-S.; Dobbins, P. A Survey of Channel Modeling for UAV Communications. *IEEE Commun. Surv. Tutorials* **2018**, *20*, 2804–2821. [CrossRef]
32. Khawaja, W.; Guvenc, I.; Matolak, D.W.; Fiebig, U.-C.; Schneckenburger, N. A Survey of Air-to-Ground Propagation Channel Modeling for Unmanned Aerial Vehicles. *IEEE Commun. Surv. Tutorials* **2019**, *21*, 2361–2391. [CrossRef]
33. Jiang, H.; Zhang, Z.; Wu, L.; Dang, J. Three-Dimensional Geometry-Based UAV-MIMO Channel Modeling for A2G Communication Environments. *IEEE Commun. Lett.* **2018**, *22*, 1438–1441. [CrossRef]
34. Bian, J.; Wang, C.-X.; Liu, Y.; Tian, J.; Qiao, J.; Zheng, X. 3D Non-Stationary Wideband UAV-to-Ground MIMO Channel Models Based on Aeronautic Random Mobility Model. *IEEE Trans. Veh. Technol.* **2021**, *70*, 11154–11168. [CrossRef]
35. Chang, H.; Wang, C.X.; Liu, Y.; Huang, J.; Sun, J.; Zhang, W.; Gao, X. A Novel Nonstationary 6G UAV-to-Ground Wireless Channel Model With 3-D Arbitrary Trajectory Changes. *IEEE Internet Things J.* **2021**, *8*, 9865–9877. [CrossRef]
36. Fu, B.; Xiao, Y.; Deng, H.; Zeng, H. A Survey of Cross-Layer Designs in Wireless Networks. *IEEE Commun. Surv. Tutorials* **2014**, *16*, 110–126. [CrossRef]
37. Available online: https://www.mathworks.com/?sïij¿tid=gnïij¿logo (accessed on 8 December 2023).
38. Available online: https://support.riverbed.com/content/support.html (accessed on 8 December 2023).
39. *IEEE Std 802.11ax-2021* ; IEEE Standard for Information Technology–Telecommunications and Information Exchange between Systems Local and Metropolitan Area Networks–Specific Requirements Part 11: Wireless LAN Medium Access Control (MAC) and Physical Layer (PHY) Specifications Amendment 1: Enhancements for High-Efficiency WLAN. Amendment to IEEE Std 802.11-2020. IEEE: Piscataway, NJ, USA, 2021; pp. 1–767. [CrossRef]
40. He, Y.; Wang, D.; Huang, F.; Zhang, R.; Gu, X.; Pan, J. A V2I and V2V Collaboration Framework to Support Emergency Communications in ABS-Aided Internet of Vehicles. *IEEE Trans. Green Commun. Netw.* **2023**, *7*, 2038–2051. [CrossRef]
41. Available online: https://fgd.gsi.go.jp/download/menu.php (accessed on 8 December 2023).
42. *IEEE 802.11g-2003*; Information Technology—Telecommunications and Information Exchange between Systems—Local and Metropolitan Area Networks—Specific Requirements—Part 11: Wireless LAN Medium Access Control (MAC) and Physical Layer (PHY) Specifications—Amendment 4: Further Higher Data Rate Extension in the 2.4 GHz Band. IEEE: Piscataway, NJ, USA, 2003.